

ESTIMATION OF S WAVES ATTENUATION IN THE CENTRAL NORTH ISLAND, NEW ZEALAND USING THE NON-PARAMETRIC GENERALIZED INVERSE TECHNIQUE (GIT).

Syuhada

ABSTRACT We used regional earthquakes records ($M_l = 2-3.8$) with the distance range of 5–55 km in order to estimate the quality factor Q of S-waves in the Central North Island, New Zealand. The non-parametric GIT method with bootstrap inversion was applied to separate the attenuation function from site and source effects. We obtained attenuation function for a set of 20 frequencies ranging between 2 and 10 Hz. The values of Q extracted from the attenuation functions provided values of strong frequency-dependent relation, $Q_s(f) = 6.15 \pm 1.22 f^{0.73 \pm 0.12}$. The low Q with strong frequency dependence obtained is consistent to that obtained for other volcanic regions.

Key words: attenuation function, quality factor, volcanic regions, S-waves

ABSTRAK Kami menggunakan seismogram dari gempa lokal ($M_l = 2-3.8$) dengan jarak hiposenter 5–55 km untuk memperkirakan faktor kualitas Q dari gelombang S di Central North Island, Selandia Baru. Metoda bootstrap inversi non-parametric GIT diterapkan untuk mendapatkan fungsi atenuasi pada 20 titik frekuensi yang terletak antara 2 sampai 10 Hz. Besaran Q yang dihitung dari fungsi atenuasi memberikan relasi $Q_s(f) = 6.15 \pm 1.22 f^{0.73 \pm 0.12}$. Hasil ini konsisten dengan penelitian tentang atenuasi yang dilakukan untuk daerah gunung api lainnya.

Kata kunci: fungsi atenuasi, faktor kualitas, daerah vulkanik, gelombang S

Naskah masuk : 11 Oktober 2010
Naskah diterima : 14 Desember 2010

Syuhada
Research Center for Physics-P2F LIPI
Kawasan Puspiptek Serpong
Email : syuh001@lipi.go.id

INTRODUCTION

In the analysis of seismic waves, attenuation studies are of great interest. Seismic attenuation can be described as the amplitude decay of seismic waves with time and distance due to anelastic and elastic processes as the waves propagate through the Earth. Attenuation effects are usually expressed by the dimensionless quantity Q (quality factor). The two main mechanisms thought to be responsible for this amplitude variation are scattering and intrinsic attenuation. Intrinsic attenuation converts the seismic energy into heat, while scattering causes redirection of the energy of the wave (e.g. Stein and Wysession, 2003). In volcanic regions, both intrinsic and scattering attenuation are important but it is difficult to distinguish the mechanism of predominant attenuation (Arevalo et al., 2003).

Seismic attenuation measurements have been conducted on several volcanoes and gave significant contributions to both geological and geophysical studies in volcanic regions. For example, the seismic attenuation structure at Rabaul volcano, Papua New Guinea, has been studied using regional earthquake data and the spectral ratio method to estimate the quality factors of P and S waves (Gudmundsson et al., 2004). Gudmundsson et al. discovered that near-surface rocks inside the caldera are relatively more attenuative than those outside the caldera, with values ranging from 15–20 in the caldera indicating the influence of fractured rocks and the presence of geothermal fluids.

In this paper, we analyze S-waves from local earthquakes recorded in the Central North Island to estimate the quality factor of S-wave. The main objective of the analysis is to evaluate the crustal properties and the main mechanisms of

attenuation beneath this region using S wave attenuation.

Study Area

New Zealand is located at the boundary between the Pacific and the Australian Plates. To the southwest of New Zealand, the oceanic crust of the Australian Plate is subducting beneath continental crust of the Pacific Plate at the Puysegur Trench (Lamarche and Lebrun, 2000). Along the Hikurangi margin of the North Island, the thin dense Pacific Plate subducts obliquely beneath the thicker lighter continental crust of the Australian Plate with a relative convergence rate of 43 mm/year (Beavan et al., 2002) (Figure 1). These two subduction margins are connected by a northeast transpressional slip movement along the Alpine Fault, which crosses New Zealand (Sutherland et al., 2006).

Oblique subduction in the northern part of New Zealand results in a region of rapid extension with extremely active volcanism and high geothermal activity (Wilson et al., 1995). The

Central North Island is characterized by the young active volcanic and high heat flow region extending from Mt. Ruapehu to White Island (e.g. Wilson et al., 1995, Eberhart-Phillips and Reyners, 2009; Stern, 2009). The Central North Island is a region under active extension with an extension rate of up to 15 mm yr⁻¹ at the Bay of Plenty, and decreasing to less than 5 mm yr⁻¹ near the southern part of the region (Eberhart-Phillips and Reyners, 2009; Stern, 2009).

Recent attenuation tomography studies show a relatively low Q_p (< 150) beneath the central part of this region at depths of 50–85 km, suggesting that there is a strong connection between volcanism and low attenuation in the shallow mantle and crust (Eberhart-Phillips et al., 2008). Eberhart-Phillips et al. (2008) suggested that the strong relation observed between low attenuation of P-waves, low V_p and high V_p/V_s is mainly governed by high temperature in this part of shallow crust related to partial melt in dikes and veins (e.g. Reyners et al., 2006).

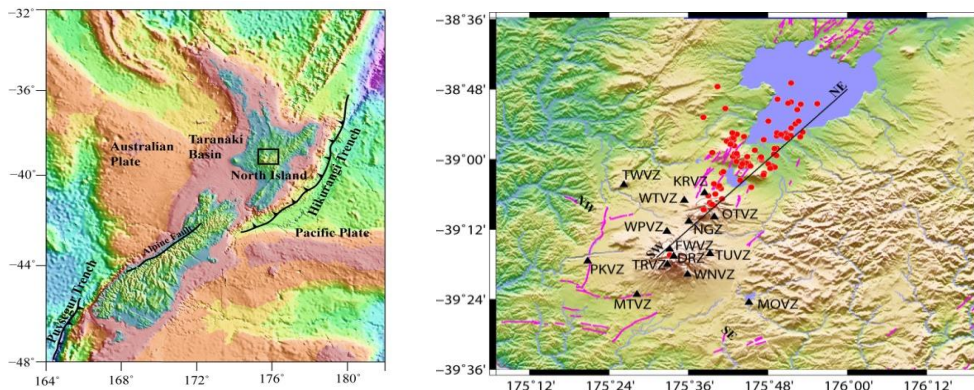


Figure 1. Left: The plate tectonic setting of New Zealand and its environs describing the interaction between the Pacific and the Australian plates (adapted after Smith and Sandwell (1997), http://topex.ucsd.edu/marine_topo/mar_topo.html). Right: The epicenters of the earthquakes used in the analysis. The black line marks the positions of the cross section shown in Fig 2.

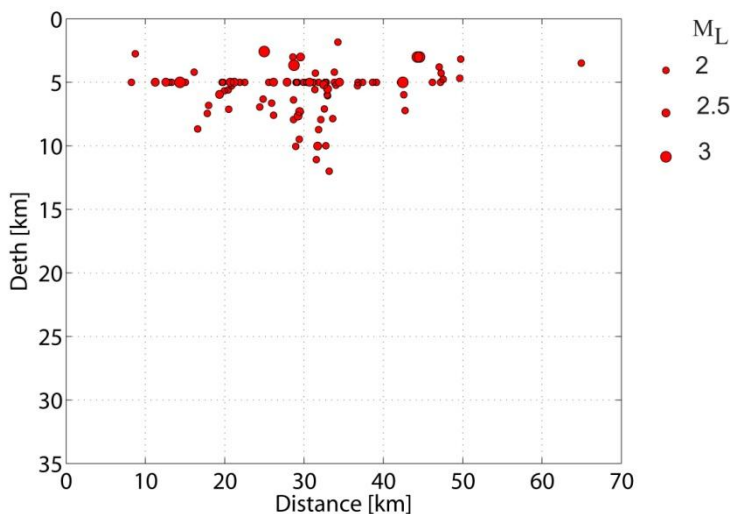


Figure 2. The vertical cross section of the earthquakes shown on the Fig. 1.

METHOD

In this study, we analyzed waveforms obtained from 90 earthquakes with magnitude ranging from $M_L=2-3.8$. The hypocentral distances of the earthquakes vary between 5 and 55 km and mostly have source depth of 5–10 km. The earthquakes distribution and the stations used in this paper are shown in Fig.1 and Fig.2. The stations are equipped with short-period and broadband seismographs recording the vertical, the north–south, and the east–west components of seismograms. The seismograms used in the analysis are all sampled at 100 samples per second with the instrument responses flat between at 1–40 Hz and 0.08–40 Hz for the short-period and broadband seismometers, respectively. In this study, only events with magnitudes of $M_L \geq 2$ with signal to noise ratio larger than 2 are retained for the inversion.

The seismograms used are baseline-corrected by subtracting the mean and removing the instrument response. In order to compute the displacement spectra, we select time windows containing clear S-wave arrivals. The initial time window starts 1 s before the S-wave arrival and ends at a time selected automatically that corresponds to the point at which 80% of the S-wave energy has been achieved. A 5% cosine taper is applied to each window before the Fourier transform calculation and the signal spectra are smoothed using the Konno-Ohmachi window (Konno and Omachi, 1998). Then, we compute the smoothed spectra at around 20 frequency points in the range 2–10 Hz. Noise spectra are calculated using P-coda windows, which have the same length as the signal windows. We use P-coda windows as noise windows because some records in our dataset have very small pre-event noise windows that preclude us from using pre-event (i.e. pre-P) noise as a noise window. Fig.3 shows sample of the displacement spectra in the east–west components.

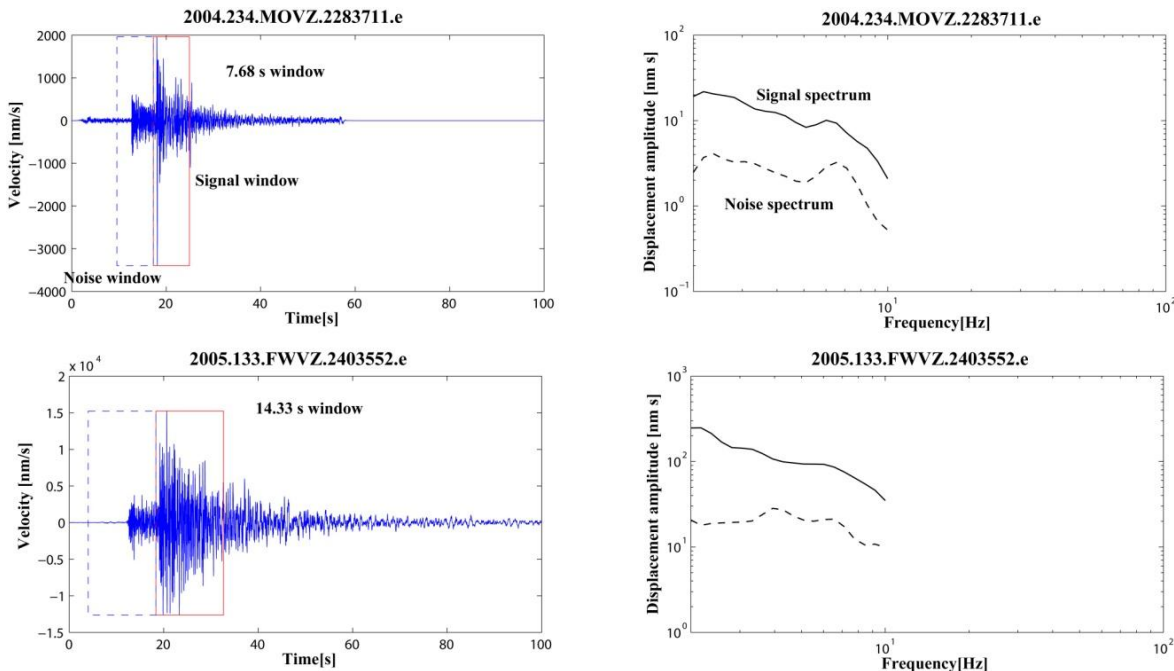


Figure 3. Left panel: Example records of the E–W component; signal and noise windows denoted by the red and blue dashed boxes respectively, used to compute the displacement spectra. Right panel: Examples of the smoothed displacement spectra obtained from the selected windows of the seismogram on the left panel.

We compute amplitude decay function with distance using the non-parametric generalized inversion (GIT) method (e.g. Castro et al., 1990). In this method, the frequency- and distance-dependence of the observed spectra are modeled as:

$$D_{ij}(f, R_{ij}) = M_i(f).A(f, R_{ij}) \tag{1}$$

Here $D_{ij}(f, R_{ij})$ is the observed spectrum of earthquake j at station i , $M_i(f)$ is a scalar, which depends on the size of the earthquake j containing both source and the average site effects (Castro et al., 1990, 2008a,b), $A(f, R_{ij})$ is related to the attenuation function (\bar{a}), whereas \bar{G}_m is a matrix related to the model space \bar{m} containing source and site terms. \bar{b} is the data vector of observed spectra. \bar{W} is a

is the attenuation function and R_{ij} is the hypocentral distance of event j to site i . We discretize the hypocentral distance ranges into 2 km bin width.

By taking the logarithm, equation 1 can be made into a linear system of equations and expressed in matrix form, as follows:

$$\begin{bmatrix} \bar{G}_a & \bar{G}_m \\ \bar{W} & 0 \end{bmatrix} \begin{bmatrix} \bar{a} \\ \bar{m} \end{bmatrix} = \begin{bmatrix} \bar{b} \\ 0 \end{bmatrix} \tag{2}$$

\bar{G}_a is a matrix representing the parameter matrix containing weighting factors w_1 chosen so that $a_1 = 0$ at $R = 0$ (reference distance) and w_2 to weight the second derivative of the curves and determine the degree of smoothness of the model

(see, e.g. Castro et al., 1990). The solution can then be obtained using least square inversion (LSQ) or singular value decomposition. The accuracy and stability of the inversion results are assessed through 200 bootstrap sample inversion for each analyzed frequency using the same procedure as reported by, for example, Oth et al. (2008).

For attenuation function obtained using equation 2, the quality factor-frequency dependence can be calculated by fitting $A(f, R_{ij})$ with the following model:

$$A(f, R_{ij}) = G(f, R_{ij}) \times e^{\frac{-\pi f R_{ij}}{\beta Q_s}} \quad (3)$$

Here $G(R_{ij})$ is the geometrical spreading function, f is the frequency, β is the shear wave velocity, Q_s is the S-wave quality factor and R_{ij} is the hypocentral distance between event j and the site i . We use an average S-wave velocity of $\beta=3.5$ km/s, based on the S-wave velocity model beneath the central of north island as obtained by Bannister et al. (2004). We define our geometrical spreading function following Castro et al. (2008b):

$$G(R) = \begin{cases} R_0 / R, & R_0 < R < R' \\ R_0 / (R' R)^{1/2}, & R \geq R' \end{cases} \quad (4)$$

We use this geometrical form to minimize the flattening effect on the amplitude decay function of the secondary arrivals of reflected waves and a change in geometrical spreading function (Castro et al., 1996). Here, R is the hypocentral distance and R' is the hypocentral distance at which the flattening effect on the amplitude decay function begins. In this study, we use $R'=25$ km (Fig 4.). R_0 is the reference distance, here chosen to be $R_0 = 5$ km; we normalize our geometrical spreading function at this distance because most

records have hypocentral distances larger than 5 km. Then, Q_s values are computed for each individual frequency. We use a model of the form (Aki, 1980a) to describe the frequency dependence of the Q :

$$Q(f) = Q_0 \left[\frac{f}{f_0} \right]^\alpha \quad (5)$$

where Q_0 is the value of Q at 1 Hz and α is the frequency-dependency coefficient.

RESULTS AND DISCUSSION

a. Attenuation function

We performed the non-parametric GIT approach to obtain attenuation functions for the regional paths of S-waves in the Central North Island, New Zealand. Figure 4 shows regional attenuation functions obtained at different selected frequencies. At low frequencies (2.58 to 4.67 Hz), the functions decrease monotonically with hypocentral distance, but a flattening effect starts to appear at around 6.02 Hz, particularly for hypocentral distances greater than 25 km. The flattening effect becomes stronger with increasing frequency.

The flattening effect apparent in the attenuation functions may reflect by several factors. Firstly, the flattening effect at $R > 25$ km may be the effect of postcritical layer reflection when the ray travels to a deeper layer of the Earth (Castro et al., 1996). An increase in velocity beneath this region might cause a similar reflection; Harrison and White (2004) deduced that a 16 km-thick quartzo-feldspathic crust is underlain to ~30 km depth beneath the Central North Island by a mafic material containing at least 2% partial melt. In contrast, Stratford and Stern (2004) reported an increase in seismic velocity for the same depth interval beneath the region and suggested that the velocity structure from 16 to 30 km depth represents the presence of anomalously low-velocity upper mantle. Another possible factor is that of reflection due to lateral variations in crustal structure (i.e. the presence of dipping interfaces).

b. The Q model

We used the attenuation functions obtained for 20 frequencies to calculate Q using equation 3. In general, the low values of Q (Fig. 5) with high frequency-dependency coefficient obtained for S-waves beneath the Central North Island agree with those found in other volcanic regions. For

example, Castro et al. (2008b) found a strong frequency dependence of Q described by the relation $Q_s = 17.8 f^{1.3}$ for a highly volcanically active region in the southern part of Italy. Styles (2009) found low S-wave Q_s of ~350 at a frequency of 10 Hz and depths shallower than 15 km in the southern part of the Central North Island.

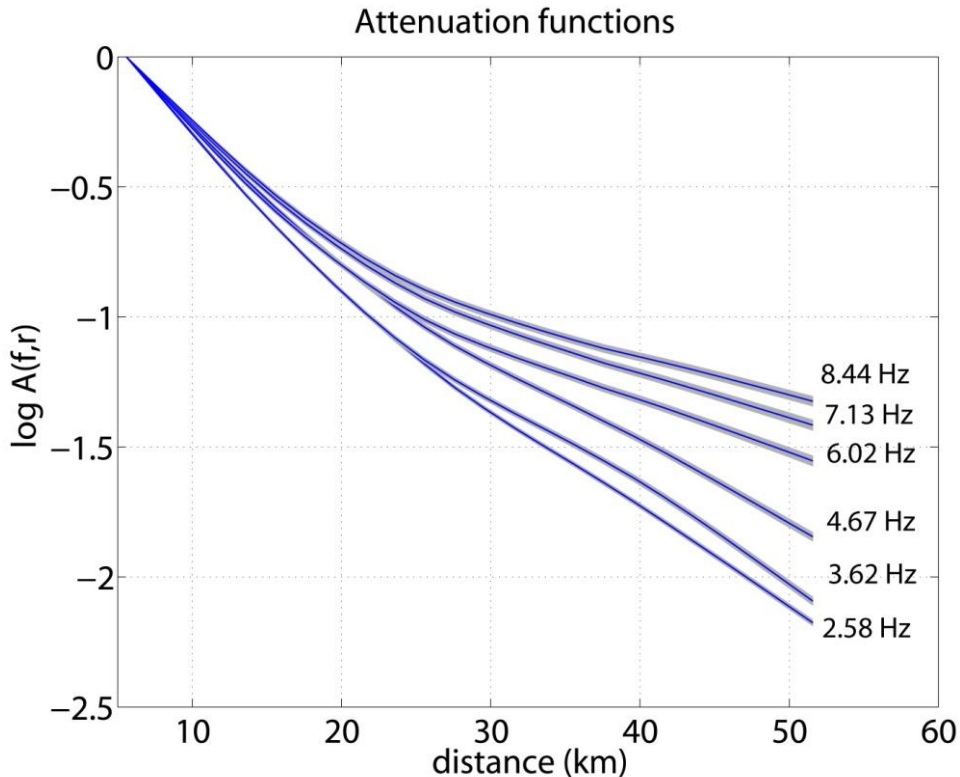


Figure 4. Spectral amplitude decay curves with distances obtained using the non- parametric GIT method at six selected frequencies. The solid line represents the mean of 200 bootstrap samples and the gray shaded area represents the mean $\pm 2\sigma$. The spectral amplitude decays faster at low frequencies than at high frequencies. The flattening effect also gets stronger with increasing frequency.

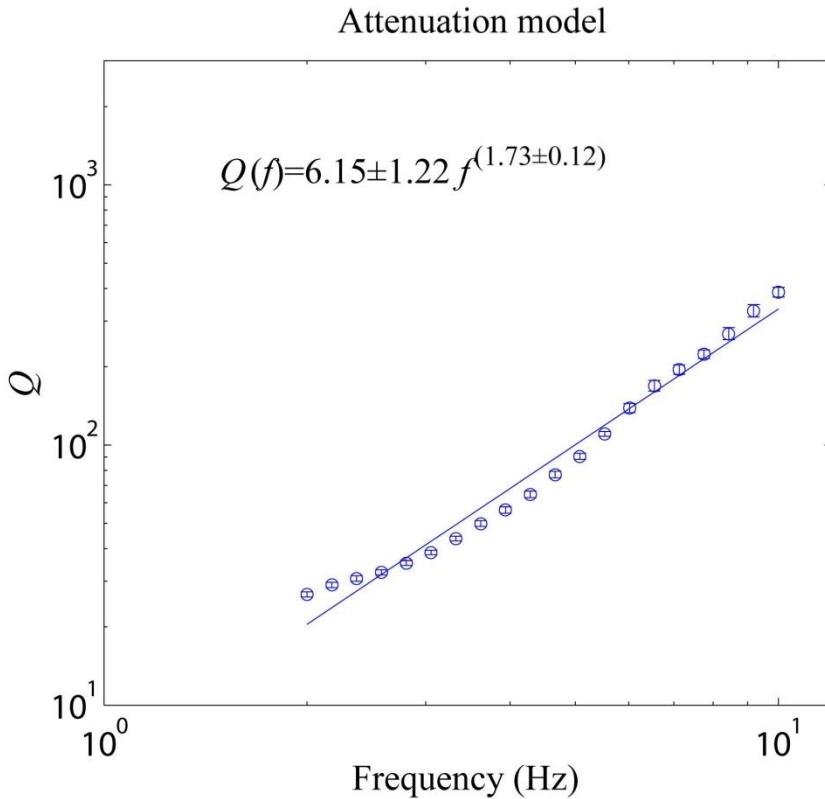


Figure 5. Estimates of Q models for S-waves obtained from seismograms in the Central North Island. The error bars denote 2σ confidence interval.

The mechanism governing frequency-dependent seismic attenuation is still unclear, although its existence has been accepted for several decades (e.g. Aki, 1980a; Kinoshita, 1994). Aki and Chouet (1975) suggested that frequency-dependent attenuation of coda waves is due to variations in backscattering processes with depth causing strong changes in Q . The frequency dependence of Q also has an important role to play in geophysical interpretation in terms of its association with tectonic activity. Numerous studies show that low Q_0 and high α are characteristic of active tectonic regions, while stable cratons are typically characterized by higher Q_0 and lower α (Aki, 1980b; Castro et al., 2008b,c).

In volcanic regions, high densities of cracks or faults may increase body wave scattering, causing lower Q with strong frequency dependence (e.g. Castro et al., 2008b), while the ductility associated with the presence of magma and hot temperatures may reduce the small-scale of heterogeneity, causing a dominance of intrinsic mechanism over scattering attenuation (Aki, 1980b; Giampiccolo et al., 2007). Intrinsic attenuation is characterized by a weaker frequency dependence of Q (Giampiccolo et al., 2007). Thus, the frequency dependence of Q can be interpreted as an indicator of the presence of hot materials and cracks, providing insights into the mechanisms governing attenuation overall.

We consider strong frequency dependence (i.e. $\alpha > 1$ (Mayeda et al., 1992)) to indicate scattering and weaker frequency dependence with $\alpha = 0.2$ to 0.3 to be caused by intrinsic attenuation (Karato and Spetzler, 1990).

However, this simple single layer model (using a whole hypocentral distance for Q estimation) does not distinguish the contributions of the upper and lower crust to the observed attenuation. We expect that waves traveling in the upper crust to be sensitive to cracks while those propagating in the lower crust to be affected by the presence of mineral fabric or partial melt. Therefore, further analysis is needed to determine the influence of the upper and lower crust on attenuation beneath the region.

CONCLUSION

The low values of Q_s exhibiting strong frequency dependence obtained within the Central North Island are comparable to those found in other volcanic regions. The frequency dependence of Q_s beneath this region suggests that scattering may dominate over intrinsic attenuation, reflecting heterogeneities within the volcanic area. Further investigation is necessary in order to substantiate the contribution of the upper and lower crust beneath this region on attenuation.

ACKNOWLEDGMENTS

I would like to thank Prof. Martha Savage and Dr. John Townend for their thoughtful discussions which provided much-needed guidance throughout this study. Many thanks go to Dr. Raul Ramon Castro who explained to me the non-paramateric GIT method. Finally, thank you to the New Zealand GeoNet project and its sponsors EQC, GNS Science and FRST for providing me with data used in this study.

REFERENCES

Aki, K., 1980a. Attenuation of Shear Waves In The Lithosphere for Frequencies from 0.05 to 25 Hz. *Phys Earth Planet In*: 21.

- Aki, K., 1980b. Scattering and Attenuation of Shear Waves in the lithosphere. *J. Geophys. Res.*, 85:6496–6504.
- Aki, K. and Chouet, B., 1975. Origin of Coda Waves: Source, Attenuation and Scattering Effects. *J. Geophys. Res.*, 80:3322–3342.
- Arevalo, C. M., Bianco, F., Ibanez, J. M., and Del pezzo, E., 2003. Shallow Seismic Attenuation and Shear Wave Splitting in The Short Period Range of Deception Island Volcano(Antarctica). *J. Volcanol. Geoth. Res.*, 128:89–113.
- Bannister, S., Bryan, C. J., and Bibby, H. M., 2004. Shear Wave Velocity Variation Across the Taupo Volcanic Zone, New Zealand, From Receiver Function Inversion. *Geophys. J. Int.*, 159:291–310.
- Beavan, J., Tregoning, P., Bevis, M., Kato, T., and Maertens, C., 2002. Motion and Rigidity of the Pacific Plate and Implications for Plate Boundary Deformation. *J. Geoph. Res.*, 107:2261.
- Castro, R. R., Anderson, J. G., and Singh, S. K., 1990. Site Response, Attenuation and Source Spectra of S Waves Along The Guerrero, Mexico, Subduction Zone. *Bull. Seism. Soc. Am.*, 80:1481–1503.
- Castro, R. R., Pacor, F., Sala, A., and Petrongaro, C., 1996. S Wave Attenuation And Site Effects in The Region of Friuli, Italy. *Bull. Seism. Soc. Am.*, 101:22355–22369.
- Castro, R. R., Condori, C., Romero, O., Jacques, C., and Suter, M., 2008a. Seismic Attenuation in Northeastern Sonora, Mexico. *Bull. Seism. Soc. Am.*, 98:722–732.
- Castro, R. R., Gallipoli, M. R., and Mucciarelli, M., 2008b. Crustal Q in southern Italy Determined from Regional Earthquakes. *Tectonophysics*, 457:96–101.
- Castro, R. R., Massa, M., Augliera, P., and Pacor, F., 2008c. Body-wave Attenuation in The Region of Garda, Italy. *Pure appl. Geophys.*, 165:1351–1366.

- Eberhart-Phillips, D. and Reyners, M., 2009. Three-dimensional Distribution of seismic anisotropy in the Hikurangi subduction zone beneath the central North Island, New Zealand. *J. Geophys. Res.*, 114:B06301.
- Eberhart-Phillips, D., Reyners, M., Chadwick, M., and Stuart, G., 2008. Three-dimensional Attenuation Structure of The Hikurangi Subduction Zone in The Central North Island, New Zealand. *Geophys. J. Int.*, 174:418–434.
- Giampiccolo, E., D’Amico, S., Patane, D., and Gresta, S., 2007. Attenuation of Source Parameters of Shallow Microearthquakes at Mt. Etna Volcano, Italy. *Bull. Seism. Soc. Am.*, 97:184–197.
- Gudmundsson, O., Finlayson, D.M., Itikarai, I., Nishimura, Y., and Johnson, W. R., 2004. Seismic Attenuation at Rabaul Volcano, Papua New Guinea. *J. Volcanol. Geoth. Res.*, 130:77–92.
- Harrison, A. J. and White, R. S., 2004. Crustal Structure of The Taupo Volcanic Zone, New Zealand: Stretching and Igneous Intrusion. *Geophys. Res. Lett.*, 31:L13615.
- Karato, S. and Spetzler, H. A., 1990. Defect Microdynamics in Minerals and solid-state Mechanisms of Seismic Wave Attenuation and Velocity Dispersion in The Mantle. *Reviews of Geophysics*, 28:399–421.
- Kinoshita, S., 1994. Frequency-dependent Attenuation of Shear Waves in The Crust of The Southern Kanto area, Japan. *Bull. Seism. Soc. Am.*, 84:1387–1396.
- Konno, K. and Omachi, T., 1998. Ground-motion Characteristics Estimated from Spectral Ratio Between Horizontal and Vertical Components of Microtremors. *Bull. Seism. Soc. Am.*, 88:1228–1241.
- Lamarche, G. and Lebrun, J. F., 2000. Transition from Strike-Slip Faulting to Oblique Subduction: Active Tectonics at The Puysegur Margin, South New Zealand. *Tectonophysics*, 316:67–89.
- Mayeda, K., Koynagi, S., Hoshihara, M., Aki, K., and Zeng, Y., 1992. A Comparative Study of Scattering, Intrinsic and Coda q for Hawaii, Long Valley, and Central California between 1.5 and 15 Hz. *J. Geophys. Res.*, 97:6643–6659.
- Oth, A., Bindi, D., Parolai, S., and Wenzel, F., 2008. S-wave Attenuation Characteristics Beneath The Vrancea Region in Romania: New Insights from The Inversion of Ground Motion Spectra. *Bull. Seism. Soc. Am.*, 98:2482–2497.
- Reyners, M., Eberhart-Phillips, D., Stuart, G., and Nishimura, Y., 2006. Imaging Subduction from The Trench to 300 km Depth Beneath The Central North Island, New Zealand, with V_p and V_p/V_s . *Geophys. J. Int.*, 165:565–583.
- Smith, W. H. F. and Sandwell, D. T., 1997. Global Seafloor Topography from Satellite Altimetry and Ship Depth Soundings. *Science*, 277:195–196.
- Stern, T. A., 2009. Reconciling Short- and Long-Term Measures Of Extension In Continental Back Arcs: Heat Flux, Crustal Structure and Rotations Within Central North Island, New Zealand. 321:73–87.
- Stein, S. and Wysession, M., 2003. An Introduction to Seismology, Earthquakes and Earth Structure. Blackwell Publishing, Oxford.
- Stratford, W. R. and Stern, T. A., 2004. Strong Seismic Reflections and Melts in The Mantle of a Continental Back-Arc Basin. *Geophys. Res. Lett.*, 31:L06622.

Styles, K. E., 2009. Shear Wave Attenuation Structure and Anisotropy in the Hikurangi Subduction Zone, Central North Island, New Zealand. PhD thesis, School of Earth and Environment, The University of Leeds, England.

Sutherland, R., Berryman, K., and Norris, R., 2006. Quaternary Slip Rates and Geomorphology of the Alpine Fault: Implications for Kinematics and Seismic

Hazard in Southwest New Zealand. Geological Society of America Bulletin, 118:464–474.

Wilson, C. J. N., Houghton, B. F., McWilliams, M. O., Lanphere, M. A., Weaver, S. D., and Briggs, R. M., 1995. Volcanic and Structural Evolution of Taupo Volcanic Zone, New Zealand: a Review. J. Volcanol. Geoth. Res., 68:1–28.